ISSN 1392 – 124X INFORMATION TECHNOLOGY AND CONTROL, 2010, Vol. 39, No. 1

COUPLING OF ZONES WITH DIFFERENT RESOLUTION CAPABILITIES IN FINITE ELEMENT MODELS OF UNIFORM STRUCTURES

Rimantas Barauskas, Vidmantas Rimavičius

Department of System Analysis, Kaunas University of Technology
Studentu Str. 50 - 407, LT-51368 Kaunas, Lithuania
e-mail: rimantas.barauskas@ktu.lt, vidmantas@achema.com

Abstract. In this paper, we describe an approach that enables to present a finite element model of a large uniform structure by an assembly of zones of different resolution capability. While actions imposed upon a structure are located in finer resolution patches, the rougher resolution zones serve as a surrounding for finer ones in order to describe the overall behavior of the structure. As an example, a fine rectangular girder construction made of beam elements is considered as a finely refined representation of the structure. The overall behavior of the structure may be considered on the base of the continuous membrane model. The structure has been created, where analyzed girder subdomain is coupled to equivalent membrane via contact elements. Criterion of mutual matching of responses of both structures is considered to be the coincidence of displacements of respective nodes in the researched subdomains of the models. The least squares method and artificial neural network approach have been employed for the identification of the physical parameters of the equivalent membrane. The efficiency of both approaches is compared. Calculations are performed in ANSYS and MATLAB environments.

Keywords: finite elements, model reduction, parameter identification.

1. Introduction

A rational combination of accuracy and efficiency of computational models may be achieved by using different modeling approaches based on a seemless joining of models made of different sizes and kinds of elements. One of the important directions in the recent development of numerical methods is referred to as multi-scale modelling. It is devoted to the correspondence of material behaviour on several levels or scales: from macro (global level, body as a whole) over mezzo and micro to nano level (molecular or atomic material structure) [6].

Multi-scale models are encountered in a wide variety of physical applications, such as mechanical, electro-magnetic, wave propagation, etc. A typical mechanical application is the dynamic modeling of response of protective textile structures and packages widely used in medicine, war industry, aviation and civil engineering. A widely used model reduction approach is based on the homogenization procedure, where the computational domain is presented by solid finite elements with material properties obtained by analysing the behavior of a typical cell of the structure [2].

When modelling complex structures, one of modelling strategies are superelements [7,8]. The main benefit of applying superelements is that calculations are performed more quicker in contrast to calculations necessary for splitting the same construction into small finite elements. While using superelements, measurements of construction equation system decrease remarkably. If the constructions contain a sufficient number of the same superelements, then the calculation time is economized. If the analyzed construction is very complex, then multidegree superelement models are compiled.

Generally, simplified (reduced) models of complex structures can be obtained on the base of comparison of their response to appropriate set of excitations against the response of a more detailed model exposed to the same excitations. The parameters of the reduced model can be adjusted by performing the minimization of error functions, quantitatively indicating the non-coincidence of the response between the simplified and reference models. An alternative approach can be based on neural network techniques in order to synthesize the models exhibiting the required structural response [10, 13].

Ballistic protection models of textiles are based on the analysis of high-velocity impact, which is concentrated in a comparatively small zone of a fabric. However, for the correct representation of the process, large pieces of cloths and packages have to be modelled [3, 4]. For this purpose, the woven structure can be represented by using models of different levels of detalization. Woven structure composed of shell elements [4], simpler and more efficient combined particles model [5], orthotropic membrane models [3], have been employed in order to represent the dynamic behavior of textile cloths under conditions of mechanical impact and penetration. A special attention and prospective deserve models in which central and distant zones of the same structure are presented by different models. As in [3], the zone of ballistic interaction of textile structure has been modeled by using the complex contact model of a woven structure, meanwhile the distant zones have been presented by membrane elements. The coupling between the zones has been implemented by means of tie constraint [3, 9]. The main purpose of this combination was to implement the "almost infinite" surrounding.

A dense girder structure has been analysed in our recent work [12], where the equivalent membrane model exhibiting similar features under static and dynamic loading has been obtained. The conformity criterion of interrelationship of the two models was assumed to be the coincidence of the corresponding nodal displacements. Displacements of all nodes of the models within the domain of size $L \times L$ have been taken into account when formulating the optimization task, during which the parameter identification of the membrane was performed. In this work, the further development of the approach is presented. The girder structure has been employed as a small patch in the central zone of the equivalent continuous membrane, which is used in order to present the surrounding, which should imitate a vast girder structure. We demonstrate two approaches to the construction of reduced models. One of them is based on the minimization of penalty-type target function representing the residual between the two sets of responses. The other approach employs the artificial neural network technique.

2. Problem Statement

In this analysis, the girder structure consists of 2D rectangular grid frame elements (see Figure 1a). The overall analysed model presents the membrane and a small girder subdomain $L_m \times L_m$ (see Figure 1b) integrated into it. The coupling between two different structural domains has been ensured by using contact elements as penalty functions. The aim to achieve was to ensure that the behaviour of $L_m \times L_m$ membrane subdomain under the mechanical loads imposed on it resembles as much as possible the behavior of the overall girder structure. The size of the membrane elements was allowed to be bigger than the cell of the girder. The criterion of the equivalency of the two models was the coincidence of the corresponding nodal displacements within the $L_m \times L_m$ girder subdomain.

Consider rectangular membrane and rectangular girder which have identical dimensions of the size $L \times L$ (see Figure 1). The girder geometry is described by rod width h, rod thickness b and the number of cells N_g along the side of the girder. Physical parameters used in the small displacement elasticity model are Young's module E_g and mass density ρ_g. The membrane model is characterized by thickness s_m, Young's module E_m, Poisson's ratio ν_m, shear module G_m, mass density ρ_m and the number of cells N_m along the side of the membrane. Membrane parameters ν_m, E_m, G_m and s_m have to be established, which enable the membrane to exhibit the same or similar behaviour in terms of displacements of respective element nodes at a given loading.

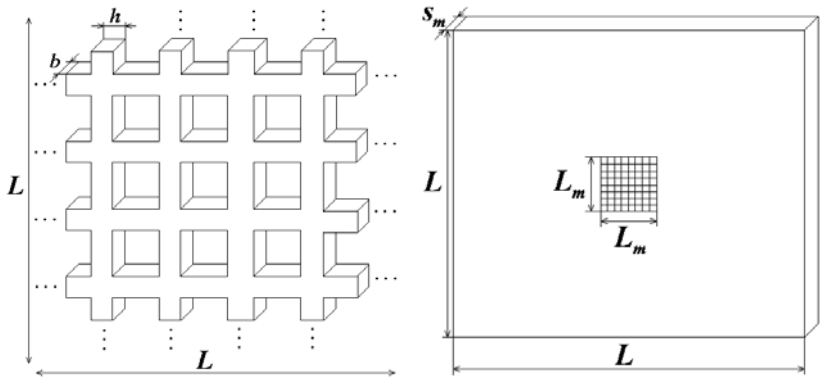

a) b)

Figure 1. The girder (a) and equivalent membrane with integrated girder (b)

As a measure of quality of the approximation of the girder model by equivalent membrane model we employ the minimum of the penalty-type target function expressed as a sum of squares of differences between the displacements of the corresponding nodes of each model. The static as well as dynamic

behaviour of the two structures has been analyzed. The schemes of four static loading cases are presented in Figure 2, where all structures have been exposed to static load F and the differences of displacements of $L_m \times L_m$ subdomain selected nodes have been included into the penalty function expression.

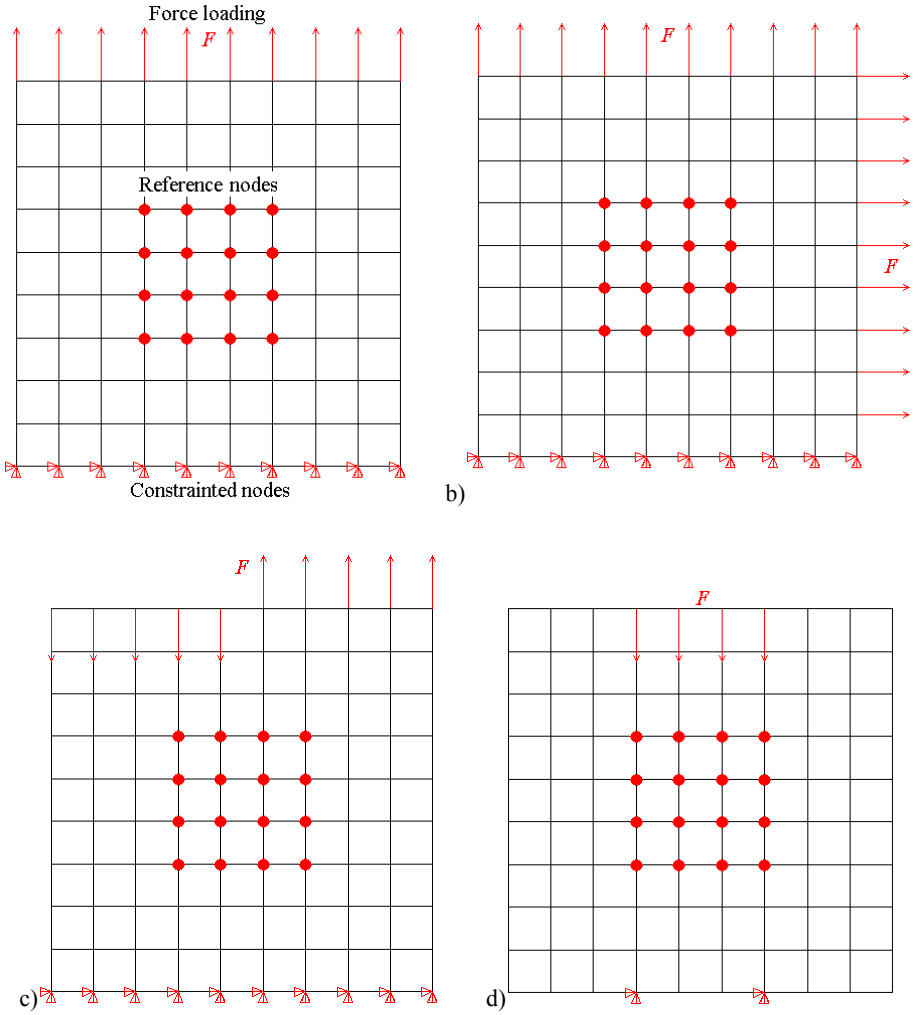

Figure 2. The finite element models: a) 1st analysis model; b) 2nd analysis model;c) 3rd analysis model; d) 4th analysis model

The analysis has been performed by using ANSYS and MATLAB software. The displacements obtained in ANSYS have been used when forming the target function, which subsequently has been minimized by employing MATLAB function FMINCON(). Distinct element structures are coupled via contact elements in membrane, moreover, these elements are realized by commands CONTA171 and TARGE169 in ANSYS program.

The obtained parameters of the equivalent membrane shall be tested by using 2nd and 3rd analysis models (see Figure 2b) and c)) and freely selected test model (loading case), which is presented in Figure 3. Also the obtained parameters of the equivalent membrane shall be tested and compared with the obtained equivalent membrane parameters of artificial neural network (ANN), where MATLAB function TRAINLM() has been used.

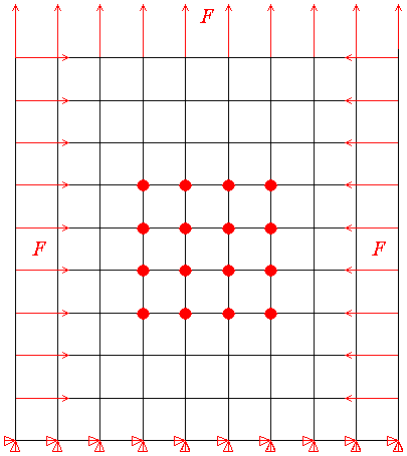

Figure 3. The test model

In the case of dynamic analysis, the differences between displacements of $L_m \times L_m$ subdomain nodes

are minimized in all analysis models at selected time moments.

The approach of genetic algorithms [15, 16] or global optimization [1, 14] would be mostly suitable for the optimization of a function with many variables and local extremes. These optimization approaches should be used in those cases, where the best solution is not necessary and only a close one is required. When the optimization theory is used, mathematical programming approaches must be applied for solving, for example, a minimization task, and this task must be described by mathematical expressions. They also should be used in order to describe the properties of the modeled object. The mathematical model includes the objective function, expressing the selected criterion of optimization, and various restrictions for the solution of the analyzed problem. Solution of the problem obtained by using chosen optimization approach gives the relatively optimal solution, but none of the optimization approaches may guarantee „the most optimal" solution [14].

3. Analysis of Results

3.1. Static analysis

In order to simplify the optimization problem assume $E_g = E_m$, $\nu_m = 0$, $\rho_g = \rho_m$ and $h = b$. Assume the girder rods being thin enough to maintain the mechanical features of a girder as

$$\frac{L}{20 \cdot N_g} \le b \le \frac{L}{8 \cdot N_g}, \tag{1}$$

where L is the side length of the rectangular element and N_g – the number of cells along the side of the girder.

In this example the number of cells in the membrane mesh is much bigger in comparison to the girder mesh.

Consider the models in Figure 2. In the first load case (LC1) (see Figure 2a), all nodes of the bottom side are fixed, meanwhile all nodes of the top side are exposed to forces imitating distributed loading along the *Oy* direction. In the second load case (LC2) (see Fig. 2b), the top side is exposed to distributed loading along the *Oy* direction and the right-hand side is exposed to distributed loading along the *Ox* direction.

The target function is read as follows:

$$T(p_j^i, q_j^i) = \sum_{j=1}^{m} \frac{\sum_{i=1}^{n} (\vec{p}_j^i - \vec{q}_j^i)^2}{\sum_{i=1}^{n} (\vec{p}_j^i)^2 + \sum_{i=1}^{n} (\vec{q}_j^i)^2}, \tag{2}$$

where p_j^i is the vector of i-node displacements of the j-model of membrane, q_j^i is the vector of i-node displacements of the j-model of girder, $n = (N+1)^2$ is the total number of the nodes of each model, N is the number of cells along the side of the subdomain $L_m \times L_m$, m is the number of the models.

After the minimization of (2), we obtained the relationship of optimum thickness s_m of the equivalent membrane against the girder rod thickness b and against the shear module G_m. Inaccuracy estimation Δ in percentage between the girder and its equivalent membrane has been found. The analytical expressions of the relationship read as:

$$s_m = 1.2249 \cdot b^2 \cdot N_g - 0.0017 \cdot b,$$

$$G_m = 9.5710 \cdot 10^{10} \cdot b^2 \cdot N_g^2, \tag{3}$$

$$\begin{aligned}
\Delta = {} & 1.9230 \cdot 10^7 \cdot b^3 + (7.6940 \cdot b - 1.2908 \cdot \\
& \cdot 10^4 \cdot b^2 - 1.9338 \cdot 10^6 \cdot b^3) \cdot N_m + \\
& + \left(2.0459 \cdot 10^3 \cdot b^2 - 0.4150 \cdot b\right) \cdot N_m^2 + \\
& + \left(0.0142 \cdot b - 59.1597 \cdot b^2\right) \cdot N_m^3 + \\
& + (0.0056 + 1.4129 \cdot 10^4 \cdot b^2 - \\
& 3.2840 \cdot 10^6 \cdot b^3 + (4.8692 \cdot 10^5 \cdot b^3 - \\
& - 1.9426 \cdot 10^3 \cdot b^2) \cdot N_m - 1.9240 \cdot 10^4 \cdot b^3 \cdot \\
& \cdot N_m^2 + (1.5339 \cdot b^2 + 443.8710 \cdot b^3) \cdot N_m^3) \cdot \\
& \cdot N_g + (7.6239 \cdot 10^4 \cdot b^3 - 484.5303 \cdot b^2 + \\
& + (85.0456 \cdot b^2 - 0.0302 \cdot b - 1.0847 \cdot 10^4 \cdot b^3) \cdot \\
& \cdot N_m + (8.5814 \cdot 10^{-4} \cdot b - 2.8725 \cdot 10^{-7} - \\
& - 1.7116 \cdot b^2 + 419.8504 \cdot b^3) \cdot N_m^2 + \\
& + (4.888 \cdot 10^{-9} - 1.8221 \cdot 10^{-5} \cdot b - 13.9707 \cdot b^3) \cdot \\
& \cdot N_m^3) \cdot N_g^2 + (4.1730 \cdot b^2 - 350.2207 \cdot b^3 + \\
& - (2.4836 \cdot 10^{-4} \cdot b - 0.6622 \cdot b^2) \cdot N_m + \\
& + (4.8652 \cdot 10^{-6} \cdot b + 0.0074 \cdot b^2 + 1.5875 \cdot b^3) \cdot N_m^2 + \\
& + 0.0727 \cdot b^3 \cdot N_m^3) \cdot N_g^3.
\end{aligned}$$

Formula (3) is correct if $b, N_g, N_m \neq 0$.

The deviations of calculated optimum values of the membrane parameters with respect to obtained formula (3) have been evaluated as

$$\Delta_i = \frac{n \cdot \sqrt{(p_x^i - q_x^i)^2 + (p_y^i - q_y^i)^2}}{\sum_{i=1}^{n} (|q_x^i| + |q_y^i|)}, \tag{4}$$

where n is the total number of nodes of each model, p_x^i, p_y^i are x and y displacements of node i of the membrane, q_x^i, q_y^i are x and y displacements of node i of the girder.

By using the artificial neural network approach, we intended to obtain the properties of the equivalent membrane and compare them to the equivalent membrane against the ones produced by formula (3).

The backpropagation ANN has been generated and taught by applying 105 girders and vector values of

the equivalent membrane. Vector pairs are obtained by applying MATLAB algorithm function FMINCON() of nonlinear optimization, i.e. optimal three-dimensional vector output value has been obtained for each respective input value of three-dimensional vector. The optimization process was performed by minimizing girder and membrane element nodes' displacements. The input vector is $\vec{x} = \begin{bmatrix} N_m & b & N_g \end{bmatrix}^T$. The output vector is $\vec{y} = \begin{bmatrix} s_m & G_m & \Delta \end{bmatrix}^T$, where Δ is the inaccuracy estimation between the girder and the equivalent membrane.

We composed the ANN with one hidden layer (see Figure 4), and carried out the selection of the number of artificial neurons in the hidden layer.

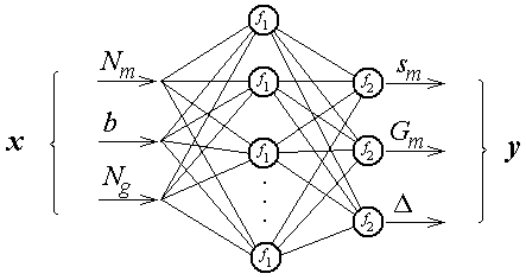

Figure 4. The ANN with one hidden layer

We have also chosen and tested the transfer (activation) function 'transig' and ,logsig' of artificial neural network hidden layer. A linear transfer function was used in the output layer.

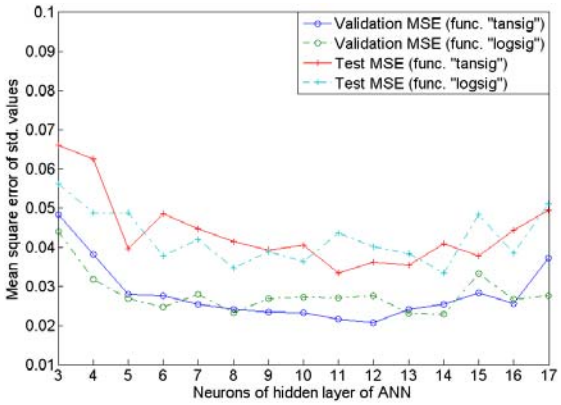

Figure 5. Selection of the number of neurons in the hidden layer of ANN and transfer function

From the results of the analysis in Figure 5 it could be noted that there are 11 neurons in the artificial neural network of the hidden layer, where transfer function ,transig' was used. Further, the selected structure of the ANN was used for the static analysis.

Moreover, we present the performance examples of models built on the base of the derived dependencies (3). The number of divisions along the side of validation models was $N_g = 42$, and the value b of the girder was chosen in accordance with the formula $b = \frac{L}{8 \cdot N_g}$. The parameters of equivalent membrane have been calculated according to formula (3) and the number of cells along the side of the membrane was $N_m = 36$. The same loading of the model has been used in all investigated cases as in Figure 2 b) and c). The estimation of the deviations of equivalent membrane displacements from the reference displacements of the girder is presented in Figure 6.

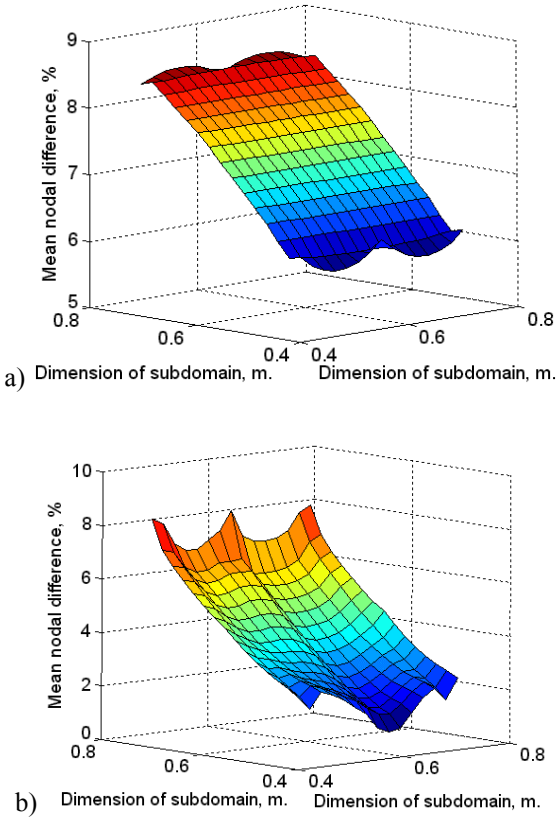

Figure 6. The estimated values of differences of displacements of the corresponding nodes of equivalent membrane (calculated by formula (3)) and girder by using 2nd (a) and 3 rd(b) models (Figure 2)

After calculation according to formula (3), the inaccuracy estimation is $\Delta = 5.3\%$. However, during the experiment the values of the inaccuracy estimation were slightly bigger. In the course of application of the 2nd model, the inaccuracy estimation amounts to 8.6% (see Figure 6a). In the course of application of the 3rd model, the inaccuracy estimation decreased to 8.2% (see Figure 6b).

Thereinafter, we have carried out the analysis with the same girder and equivalent membrane, physical features of which were calculated by the ANN. Comparison test was applied to the same 2nd and 3 rd (see Figure 2 b) and c) models. Model estimations are presented in Figure 7.

Having calculated the inaccuracy estimation by artificial neural network, we obtain $\Delta = 5.2\%$. However, comparing Figure 6 and Figure 7 it could be noticed that slightly smaller values are reached with the ANN. The inaccuracy of the 2nd model amounts to 6.6% and that of the 3rd model is 7.1%.

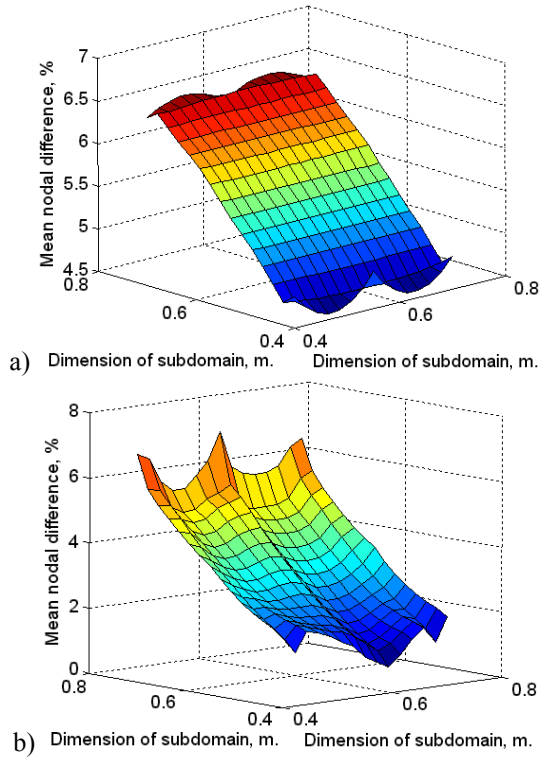

Figure 7. The estimated values of differences of displacements of the corresponding nodes of equivalent membrane (calculated by ANN) and girder by using 2nd (a) and 3rd(b) models (see Figure 2)

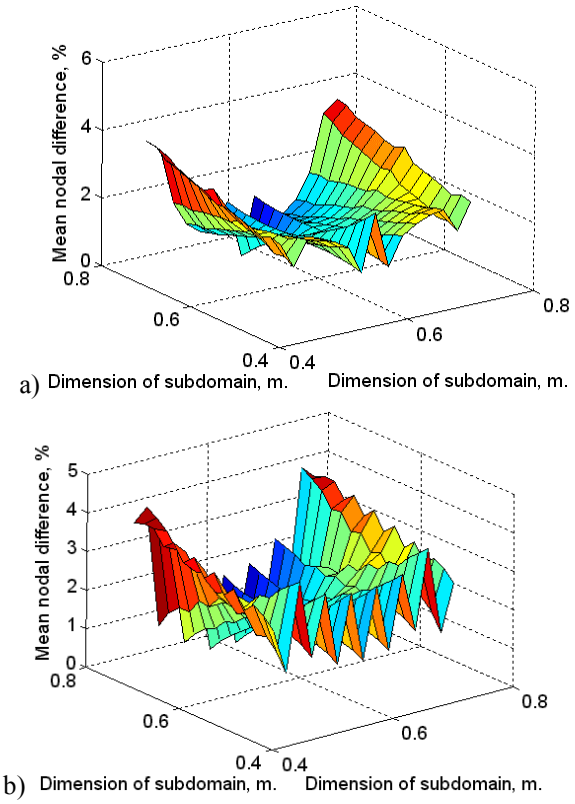

Figure 8. The estimated values of differences of displacements of the corresponding nodes of equivalent membrane (calculated by formula (3)) and girder by using test model (see Figure 3), where a) N_m= 32 and b) N_m= 21

Further, we have chosen test model (see Figure 3) and then calculated physical parameters of the equivalent membrane by applying formula (3). Estimations of test model girder (Ng = 42) and equivalent membrane are presented in Figure 8.

The maximum value of the test model inaccuracy amounts up to 4.2% (see Figure 8a). In case when equivalent membrane mesh is enlarged half the size, the inaccuracy value increased up to 4.8% (see Figure 8b).

This test model has also been analysed in the situation where equivalent membrane physical features were calculated by the ANN. The analysis results are provided in Figure 9.

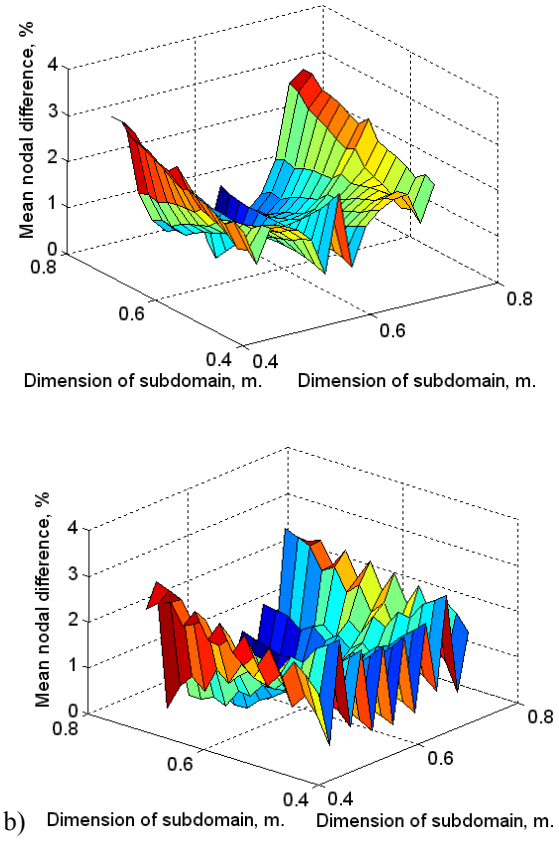

Figure 9. The estimated values of differences of displacements of the corresponding nodes of equivalent membrane (calculated by ANN) and girder by using test model, where a) $N_m = 36$ and b) $N_m = 21$

The maximum inaccuracy value of test model amounts to 3.2% (see Figure 9a), where the parameters of the equivalent membrane were calculated by the artificial neural network. If equivalent membrane mesh is enlarged half the size, the maximum value increases up to 3.5% (see Figure 9b), and the differences between 3D graph have become more significant.

3.2. Dynamic analysis

In this section we extended the formulas, as determined in Section 3.1 for the static analysis, to the dynamic analysis. Time is introduced as continuous variable $t \in [0;T]$ and optimization is performed by

using a new target function obtained through integrating expression (2) over time. Now the nodal displacements are stored at all time steps t_k. The integration over time is performed numerically by using the 5th order of Newton – Cottes quadrature formula [11].

The time law of the loading is expressed by $T \approx L\left(\frac{E_g}{\rho_g}\right)^{-\frac{1}{2}}$. We chose the time interval of the transient dynamic analysis to be equal to the time necessary for the longitudinal elastic wave in order to travel distance L equal to the side length of the model.

Forces at the individual nodes have been calculated in accordance with $F = \frac{2 \cdot F_{\max} \cdot \sin(\pi \cdot t)}{2 \cdot N - 1}$ to have the period $T_F \approx \frac{T}{2}$ (see Figure 10b). In order to imitate the distributed loading of the side of the membrane, the nodes at vertices of the rectangular membrane are affected by only half of the force, which is applied to other nodes of the membrane boundary.

Optimization was carried out in statics and dynamics against the models presented in Figure 2. Moreover, we select all reference nodes of the subdomains $L_m \times L_m$ (see Figure 2a), at which displacement of both structures are compared against each other. In order to carry out the process of minimization we use the FMINCON() function. After the minimization of (2), we obtained the relationship between the girder and the equivalent membrane. The analytical expressions of the relationships between the geometric parameters of the girder and the equivalent membrane have been established and the expressions are expressed by:

$$
\begin{aligned}
s_m &= 1.2249 \cdot b^2 \cdot N_g - 0.0017 \cdot b, \\
G_m &= 9.5710 \cdot 10^{10} \cdot b^2 \cdot N_g^2, \qquad (5) \\
\rho_m &= 2.3691 \cdot 10^4 + 9.1144 \cdot 10^5 \cdot b + 1.5173 \cdot \\
&\cdot 10^8 \cdot b^2 - 624.4767 \cdot N_m + 17.8909 \cdot N_m^2 + \\
&(6.3177 \cdot 10^3 \cdot b^2 - 27.4322 \cdot b - 0.1427) \cdot \\
&\cdot N_m^3 - 2.4356 \cdot 10^7 \cdot b^2 \cdot N_m - (5.2866 \cdot 10^5 \cdot \\
&\cdot b^2 - 664.5475 \cdot b) \cdot N_g^2, \\
\Delta &= 0.7163 - 18.949 \cdot b + (3.0841 \cdot b - 0.0206) \cdot \\
&\cdot N_m + (3.152 \cdot 10^{-4} + 44.9452 \cdot b^2) \cdot N_m^2 + \\
&(2.3679 \cdot b + 560.2237 \cdot b^2 - (0.1537 \cdot b + \\
&+ 118.6175 \cdot b^2) N_m - 0.9973 \cdot b^2 \cdot N_m^2) \cdot N_g + \\
&+ (3.0879 \cdot b^2 \cdot N_m - 0.0973 \cdot b) \cdot N_g .
\end{aligned}
$$

Formula (5) is correct if $b, N_g, N_m \neq 0$.

Furthermore, a backpropagation artificial neural network has been made up and taught by applying 105 vector values (sample), obtained through optimization of membrane under selected girder. Next, vector pairs are obtained through the FMINCON()function of optimization in MATLAB environment, i.e. each value of the input 3D vector corresponds to the optimal value of output 4D vector. The optimization process was performed by minimizing girder and membrane element nodes‘ displacements. The input vector is $\vec{x} = \left[N_m \quad b \quad N_g \right]^T$. The output vector is $\vec{y} = \left[s_m \quad G_m \quad \rho_m \quad \Delta \right]^T$.

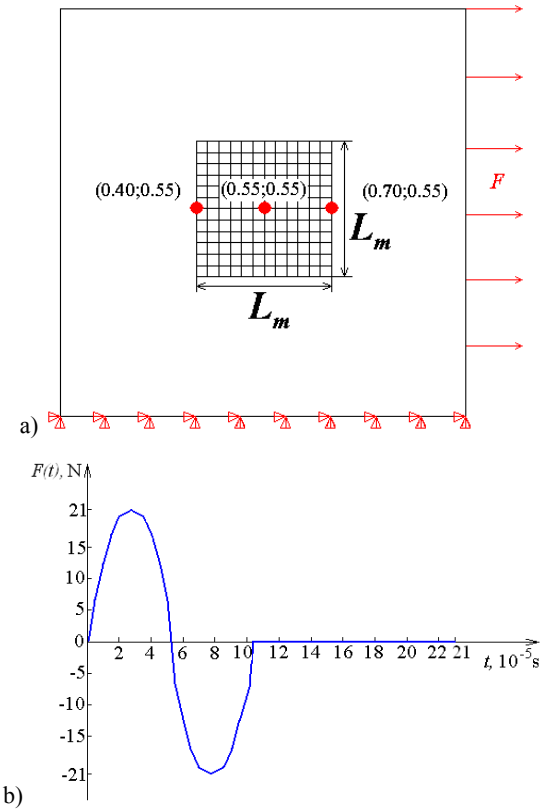

Figure 10. a) The reference nodes of the model, b) The time law of the loading force

Both in statics and dynamics analysis we made an ANN with one hidden layer and carried out selection of the number of neurons in the hidden layer (see Fig. 11). We also select the transfer functions ‚tansig‘ and ‚logsig‘ of the hidden layer. A linear transfer function was used in the output layer.

As seen in Figure 11, it could be noted that there are 9 neurons and the transfer function ‚transig‘ is used in the hidden layer of the artificial neural network. In dynamic mechanical loads the hidden layer of the artificial neural network contains 2 neurons less in comparison to the ANN in static mechanical loads. Moreover, optimal transfer function ‚tansig‘ was chosen both in statics and dynamics.

The analytic expressions are to be tested according to the model of Figure 10a. We select 3 reference nodes (see Figure 10a), at which displacement time laws of both structures are compared against each other. The mesh of size 42x42 in both structures is

employed. Figure 12 presents the magnitudes of displacements caused by the transient vibration process (the wave traveling along the *Ox* direction, (see Fig. 10a) at several selected time moments in the girder and equivalent membrane structure. The two graphs are practically equivalent to each other. Figure 13 presents errors of displacements of reference nodes. In graphs (see Figure 12), 1g, 2g, 3g denote the girder control nodes and their coordinates (see Figure 10a), and 1m, 2m, 3m stand for respective control nodes of the equivalent membrane.

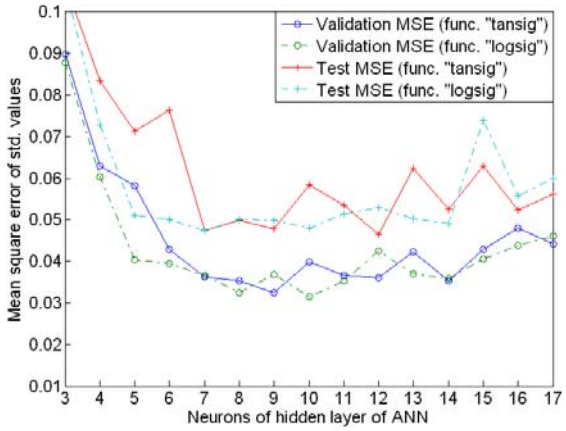

Figure 11. Selection of the number of neurons and the transfer function in the hidden layer of ANN

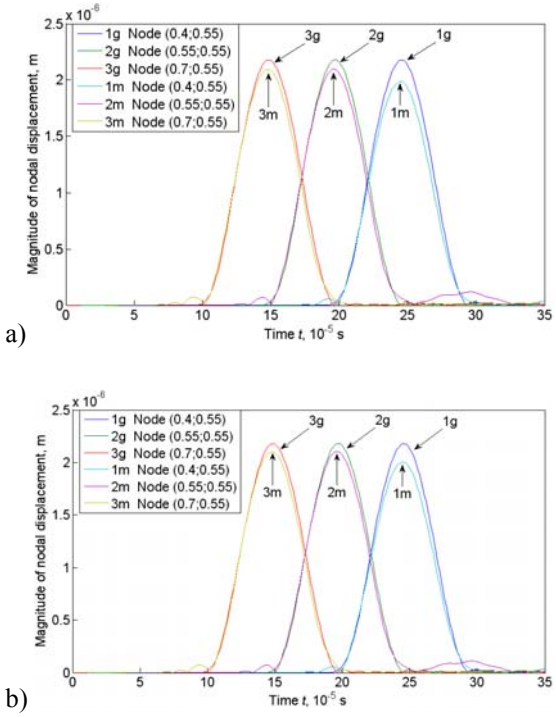

Figure 12. The magnitudes of displacements at several selected time moments in the girder and equivalent membrane structure (a) calculated by formula (5), b) calculated by ANN), $N_g = N_m = 42$

According to formula (5), we obtain $\Delta = 13\%$ through the calculation of the inaccuracy estimation. However, it could be noticed (Figure 13a) that during the experiment the maximum value is 9.7%. The inaccuracy estimation calculated by the artificial neural network is $\Delta = 11.6\%$, and the maximum value is 8.5% during the experiment (see Figure 13b).

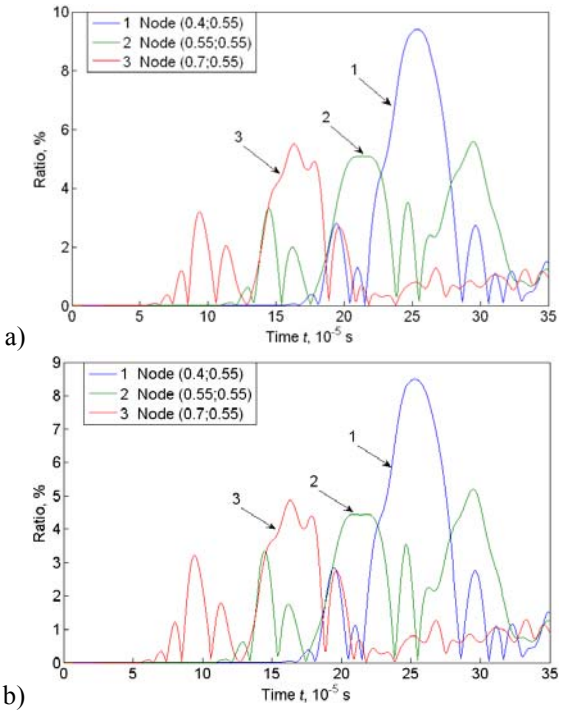

Figure 13. Differences between corresponding displacements of reference nodes of the girder and equivalent membrane model (a) calculated by formula (5), b) calculated by ANN), $N_g = N_m = 42$

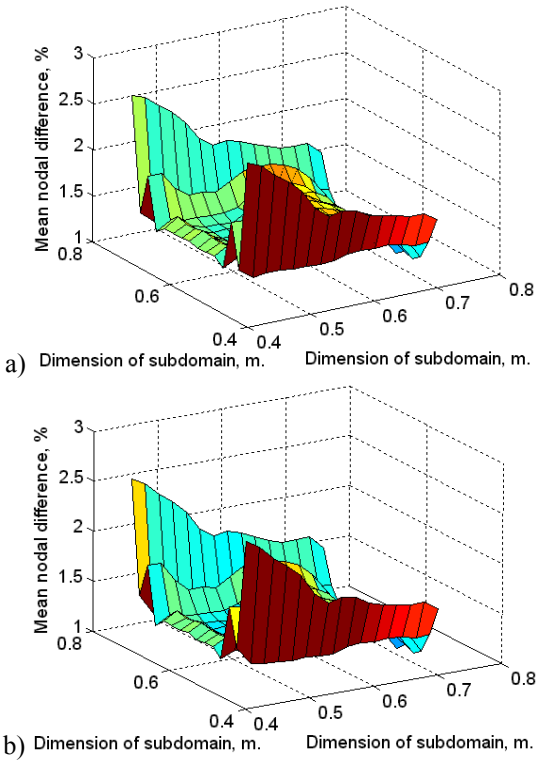

Figure 14. Differences between corresponding displacements of $L_m \times L_m$ subdomain of the girder and equivalent membrane model structure (a)calculated by formula (5), b) calculated by ANN), $N_g = 42$, $N_m = 42$

Figure 14 presents the inaccuracy of the test model subdomain $L_m \times L_m$. The values between the girder and its equivalent membrane are not high.

Figures 14a) and 14b) are very much alike in their form and values. Therefore the difference between values of absolute dimension is provided in Figure 15. The difference is not very significant and the maximum value amounts up to 0.14%.

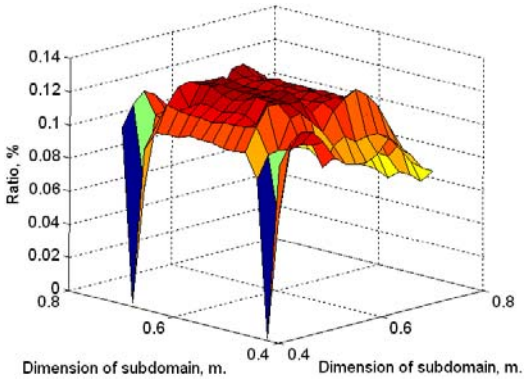

Figure 15. Differences of absolute values from Figure 14a) and Figure 14b)

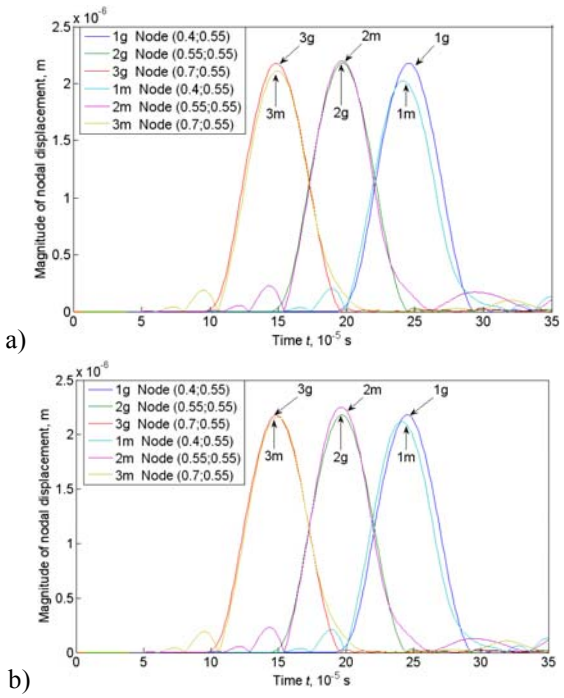

Figure 16. The magnitudes of nodal displacements of the girder and equivalent membrane structure (a) calculated by formula (5), b) calculated by ANN), $N_g = 42$, $N_m = 21$

The next numerical experiment is performed under the same model and under the same conditions, taking into consideration that the number of cells along the side of the girder is $N_g = 42$ and the number of cells along the side of the equivalent membrane is $N_m = 21$. Figure 16 presents the magnitudes of displacements caused by the transient vibration process (the wave traveling along the *Ox* direction (see Figure 10a)) at several selected time moments in the girder and equivalent membrane structure.

The wave propagation in the selected girder is very close to the wave propagation in the equivalent membrane (see Figure 16). The difference of the displacement of control nodes is presented in Figure 17.

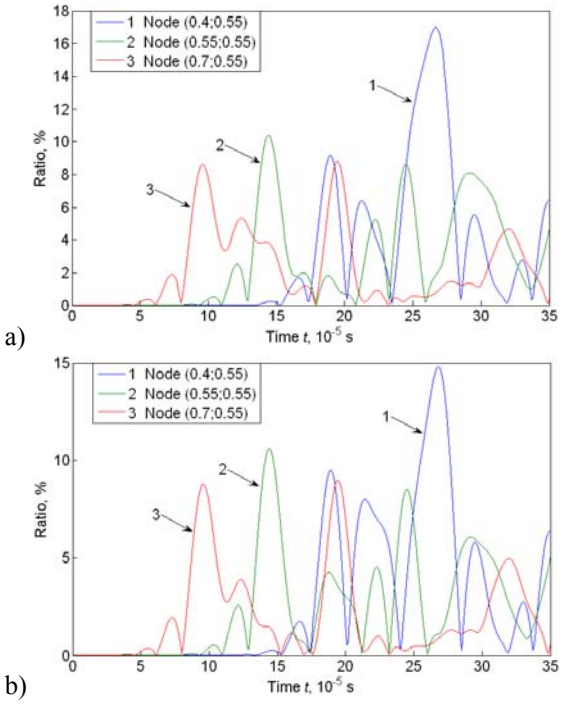

Figure 17. Differences between corresponding displacements of reference nodes of the girder and equivalent membrane model (a) calculated by formula (5), b) calculated by ANN), $N_g = 42$, $N_m = 21$

We obtained the inaccuracy values $\Delta = 23.7\%$ calculated by formula (5) and $\Delta = 22\%$ according to calculations by the ANN. It could be noted (see Fig. 17) that the inaccuracy values were smaller in the test model. Smaller inaccuracies were obtained in the case of equivalent membrane, when the physical parameters of the membrane were calculated by the ANN. The highest inaccuracy is reached at the first control node under coordinates (0.4;0.55). This point becomes more significant since the equivalent membrane mesh is 2 times thicker than the girder mesh.

In case of change of the mesh in the equivalent membrane, the physical features of the membrane change as well. If equivalent membrane mesh becomes enlarged half the size ($N_m = 21$), then estimation values of the models increase up to 1.8 times (see Figure 18).

Though Figure 18a) and Figure 18b) are similar in their shape, their difference in absolute values amounts to 0.6% (see Figure 19).

Under the same mechanical loads the equivalent membrane, whose physical parameters were obtained with the ANN, has become closer to the selected girder in respect of its behaviour.

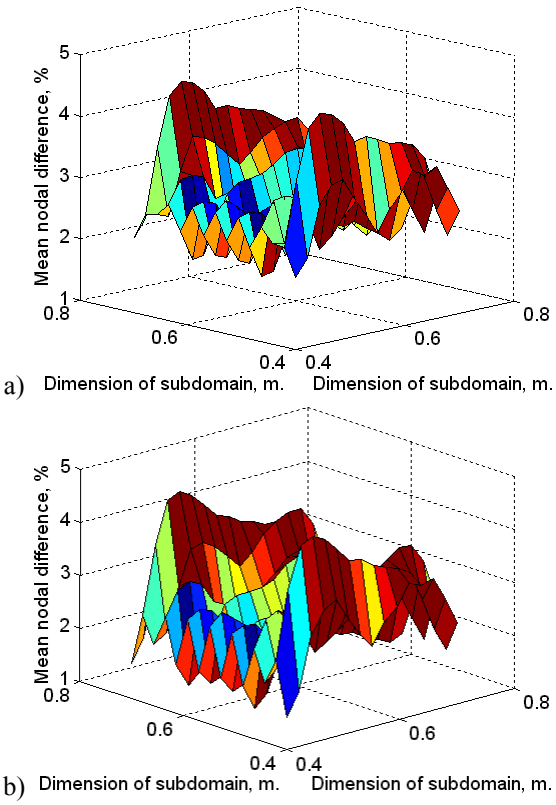

Figure 18. Differences between corresponding displacements of $L_m \times L_m$ subdomain of the girder and equivalent membrane model structure (a) calculated by formula (5), b) calculated by ANN), $N_g = 42$, $N_m = 21$

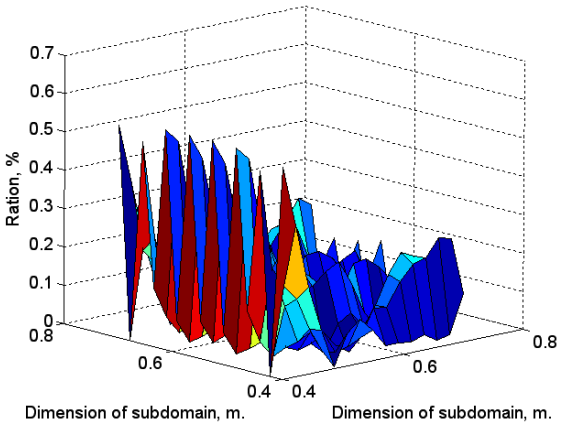

Figure 19. Differences of absolute values between Figure 18a) and Figure 18b), $N_g = 42$, $N_m = 21$

Parameters of the girder and the equivalent membrane obtained form optimization of the objective function and from artificial neural network calculations are provided in Table 1.

4. Conclusions

The continuous membrane model, which describes adequately the behavior of girder structure and can be used in the multi-scale model, has been synthesized under static, as well as, dynamic loadings. In case of static and dynamic analysis, the equivalent membrane operated satisfactorily even when the membrane element side length was twice greater than the dimension of the girder cell.

Table 1. The values of physical parameters of the girder and the equivalent membrane.

Parameter name	Formula, by which parameter is calculated	Parameter value by LSM, where $N_m = 21$	Parameter value by LSM, where $N_m = 42$	Parameter value by ANN, where $N_m = 21$	Parameter value by ANN, where $N_m = 42$
E_g ,Pa.	–	$1.5 \cdot 10^{11}$	$1.5 \cdot 10^{11}$	$1.5 \cdot 10^{11}$	$1.5 \cdot 10^{11}$
$b = h$, m.	$\frac{L}{8 \cdot N_g}$	0.00267857143	0.00267857143	0.00267857143	0.00267857143
ρ_g, $\frac{\text{kg}}{\text{m}^3}$.	–	7800	7800	7800	7800
N_g	–	42	42	42	42
ν_m	–	0	0	0	0
E_m, Pa.	E_g	$1.5 \cdot 10^{11}$	$1.5 \cdot 10^{11}$	$1.5 \cdot 10^{11}$	$1.5 \cdot 10^{11}$
s_m, m.	$s(N_m, b, N_g)$	0.00036452	0.00036452	0.00034855	0.00036112
G_m, Pa.	$G(N_m, b, N_g)$	$1.2113 \cdot 10^{9}$	$1.2113 \cdot 10^{9}$	$1.1863 \cdot 10^{9}$	$1.2225 \cdot 10^{9}$
ρ_m, $\frac{\text{kg}}{\text{m}^3}$.	$\rho(N_m, b, N_g)$	$1.6625 \cdot 10^{4}$	$1.6104 \cdot 10^{4}$	$1.6592 \cdot 10^{4}$	$1.6147 \cdot 10^{4}$
Δ,%	$\Delta(N_m, b, N_g)$	23.71	13.03	22.97	11.72

The parameters of a finite element of the equivalent membrane were obtained on the base of the approximation by the analytical formula derived either by using the least squares method or by using artificial neural network approach. Both approaches enabled to obtain satisfactory results, however, in most cases the application of the ANN technique provided the response of the equivalent membrane closer to the response of the girder at the same mechanical loads.

The study demonstrated that the inaccuracy of the membrane model synthesized by using the least squares approximation was 3-7% greater than the predicted value. The reason of the mismatch could be that the approximation formula was derived basing on the modeling results of a small reference domain, however, the test calculations were carried out on domains of different sizes.

Created mathematical expressions are suitable only for calculation of the models researched in this work. In order to make mathematical expressions suitable also for the other models, these models should be included in the scope of the original optimization task whose solution will give updated mathematical expressions. However, this would extend the possible application of mathematical expressions, but also contribute to reducing the calculation (matching) accuracy of the physical parameters of the equivalent membrane. Anyway, the variety of structures, on which the approximation rule is synthesized, should reflect as much as possible the essence of the class of the analysed problems.

References

[1] **C.S.Adjiman, I.P.Androulakis, C.A.Flaudas.** Global optimization of mixed-integer nonlinear problems. AIChE J. 46, 2000, 1769-1797.

[2] **Y.A. Bahei-El-Din, A.M. Rajendran, M.A. Zikry.** A material model for multi-scale analysis of textile composites. 44*th* AIAA/ASME/ASCE/AHS *Structures, Structural Dynamics and Material Conference*. 7-10 *April* 2003, *Norfolk, Virginia*, 685-690.

[3] **R. Barauskas.** Modeling of the bullet perforation of textile targets by using combined woven structure – membrane approach. *WSEAS Transactions on Information Science and Applications, Issue* 11, *Vol*.2, *November* 2005, ISSN 1790-0832, 1944-1954.

[4] **R. Barauskas, A. Abraitiene, A. Vilkauskas.** Simulation of a ballistic impact of a deformable bullet upon a multilayer fabric package. 2*nd International Conference on Computational Ballistics, WIT Press, Southmpton, Boston*, 2005, 41-51.

[5] **R. Barauskas, M. Kuprys.** Collision detection and response of yarns in computational models of woven structures. *Proceedings of* 10th *International Conference Mathematical Modeling and Analysis and* 2nd *International Conference Computational Methods in Applied Mathematics, June* 1-5, 2005, *Trakai*, *Lithuania*, 1-6.

[6] **M. Bizaca, Z.S omodji.** Finite element elastic homogenization of a textile-like material. *Annals of DAAAM & Proceedings, Annual*, 2005, 27-28.

[7] **C.G. Go, C.I. Lin, Y.S. Lin, S.H. Wu.** Formulation of super-element for the dynamic problem of a cracked plate. *Communications in Numerical Methods in Engineering. Vol*. 14, *Issue* 12, 1998, 1143-1154.

[8] **Ch. Song.** A super-element for crack analysis in the time domain. *International Journal for Numerical Methods in Engineering. Vol.* 61, *Issue* 8, 2004, 1332-1357.

[9] **R. Clegg, C.Hayhurst, J.Leahy, M.Deutekom.** Application of a coupled anisotropic material model to high velocity impact response of composite textile armour. 18th *International Symposium and Exhibition on Ballistics, San Antonio, Texas USA, November* 15-19,1999, 791-798.

[10] **C.C. Pain, C.R.E. De Oliveira, A.J.H.Goddard.** A neural network graph partitioning procedure for grid-based domain decomposition. *International Journal for Numerical Methods in Engineering. Vol*. 44, *Issue* 5, 1999, 593-613.

[11] **K. Plukas.** Numerical methods and algorithms. *Kaunas: Naujasis lankas*, 2001, ISBN 9955-03-061-5, (*in Lithuanian*).

[12] **R. Barauskas, V. Rimavičius.** Reduction of finite element models by parameter identification. *Information Technology and Control*, 2008, *Vol*.37, *No*.3, 211-219.

[13] **A. Verikas, A. Gelžinis.** Neural networks and neurals calculations. *Kaunas: Technologija*, 2003, ISBN 9955-09-433-8, (*in Lithuanian*).

[14] **J.Mockus.** Optimization and application. *Available at http://mockus.org/optimum/docj/distgt.pdf*, (*in Lithuanian*).

[15] **A.C. Schultz.** The Genetic Algorithms Archive. *The Navy Center for Applied Research in Artificial Intelligence. Available at http://www.aic.nrl.navy.mil/galist*.

[16] **R.Biesbroek.** History of genetic algorithms. *Available at http://www.estec.esa.nl/outreach/gatutor/history_of_ga.htm*.

Received September 2009.

DOI: 10.5755/j01.itc.39.1.12086